Remote Sensing of Environment 213 (2018) 206–214

Contents lists available at ScienceDirect

Remote Sensing of Environment

journal homepage: www.elsevier.com/locate/rse

Potential value of combining ALOS PALSAR and Landsat-derived tree cover data for forest biomass retrieval in Madagascar

Dinh Ho Tong Minh[a,*], Emile Ndikumana[a], Ghislain Vieilledent[b,c], Doyle McKey[d], Nicolas Baghdadi[a]

[a] Institut national de Recherche en Sciences et Technologies pour l'Environnement et l'Agriculture (IRSTEA), University of Montpellier, UMR TETIS, Montpellier, France
[b] CIRAD, UPR Forêts et Sociétés, Montpellier F-34398, France
[c] Joint Research Center of the European Commission, Bio-economy unit, Ispra I-21027, VA, Italy
[d] CEFE, University of Montpellier, CNRS, Institut d'Ecologie et Environnement, route de Mende, Montpellier 5 34293, France

ARTICLE INFO

Keywords:
Aboveground biomass
Biomass
Carbon
Madagascar
ALOS PALSAR
Landsat tree cover
REDD

ABSTRACT

Reducing carbon emissions from deforestation and degradation (REDD) requires detailed insight into how the forest biomass is measured and distributed. Studies so far have estimated forest biomass stocks using rough assumptions and unreliable data. High-resolution data and robust methods are required to capture the spatial variability of forest biomass with sufficient precision. Here we aim to improve on previous approaches by using radar satellite ALOS PALSAR (25-m resolution) and optical Landsat-derived tree cover (30-m resolution) observations to estimate forest biomass stocks in Madagascar, for the years 2007–2010. The radar signal and in situ biomass were highly correlated (R^2 = 0.71) and the root mean square error was 30% (for biomass ranging from 0 to 500 t/ha). Using our map at 25-m resolution for the entire island of Madagascar, we estimated the total above-ground forest carbon for the four years 2007, 2008, 2009 and 2010 to be 1.1173 ± 0.0304, 1.1029 ± 0.0303, 1.0916 ± 0.0301 and 1.0773 ± 0.0298 PgC, respectively. Carbon stocks were found to have decreased constantly over this period due to anthropogenic deforestation and likely also to climate change. The results are expected to serve as a more accurate benchmark for monitoring progress on REDD and to provide strong supports for current and future spaceborne missions such as ALOS-2, SAOCOM and BIOMASS.

1. Introduction

Forest biomass plays a key role in the global climate (Pan et al., 2011). However, compared to biomass in other ecosystems, forest biomass remains poorly quantified, owing to the practical difficulties in measuring stocks over broad geographic scales. Overcoming this obstacle is important, because quantifying forest biomass is essential for countries planning to participate in the Reducing Emissions from Deforestation and Degradation (REDD) program (Hufty and Haakenstad, 2011). REDD offers incentives (e.g., monetary compensation) for countries to preserve their forestland in the interest of reducing carbon emissions and thereby lessening the risk of climate change. Both above-ground and below-ground biomass are present, but above-ground biomass (AGB) is more commonly measured. In recent years, progress has been made in mapping forest biomass by using a range of remote sensing technologies (Saatchi et al., 2011; Baccini et al., 2012; Vieilledent et al., 2016). Nonetheless, these studies are limited by their dependence on optical sensors (relatively insensitive to biomass), low resolution (from 250 m (Vieilledent) to 500 m (Baccini) to 1000 m (Saatchi)) and inadequate sampling intensity. For example, the results of Saatchi et al. (2011) and Baccini et al. (2012) show strong discrepancies at the local scale and there are no evident reasons for preferring one map over the other.

Unlike passive optical sensors, radar systems are capable of producing high quality images of the earth even in cloud cover conditions. Synthetic aperture radar (SAR) allows for continuous global spatial coverage and systematic acquisitions, both of which are essential for constructing relevant temporal series. The potential of SAR for forest biomass estimation has been highlighted since the early 1990s (Le Toan et al., 1992). Radar intensity depends on the overall geometrical and dielectric features of these various scatterers, whose geometrical volume and wood density give the whole forest biomass. As a general rule, increasing intensity values goes with increasing biomass whether at L or P-bands, until a saturation value, which occurs earlier at L-band (Dobson et al., 1992).

The L-band ALOS mission is considered pioneering in the systematic

* Corresponding author.
E-mail address: dinh.ho-tong-minh@irstea.fr (D. Ho Tong Minh).

https://doi.org/10.1016/j.rse.2018.04.056
Received 8 August 2016; Received in revised form 16 August 2017; Accepted 28 April 2018
Available online 19 May 2018
0034-4257/

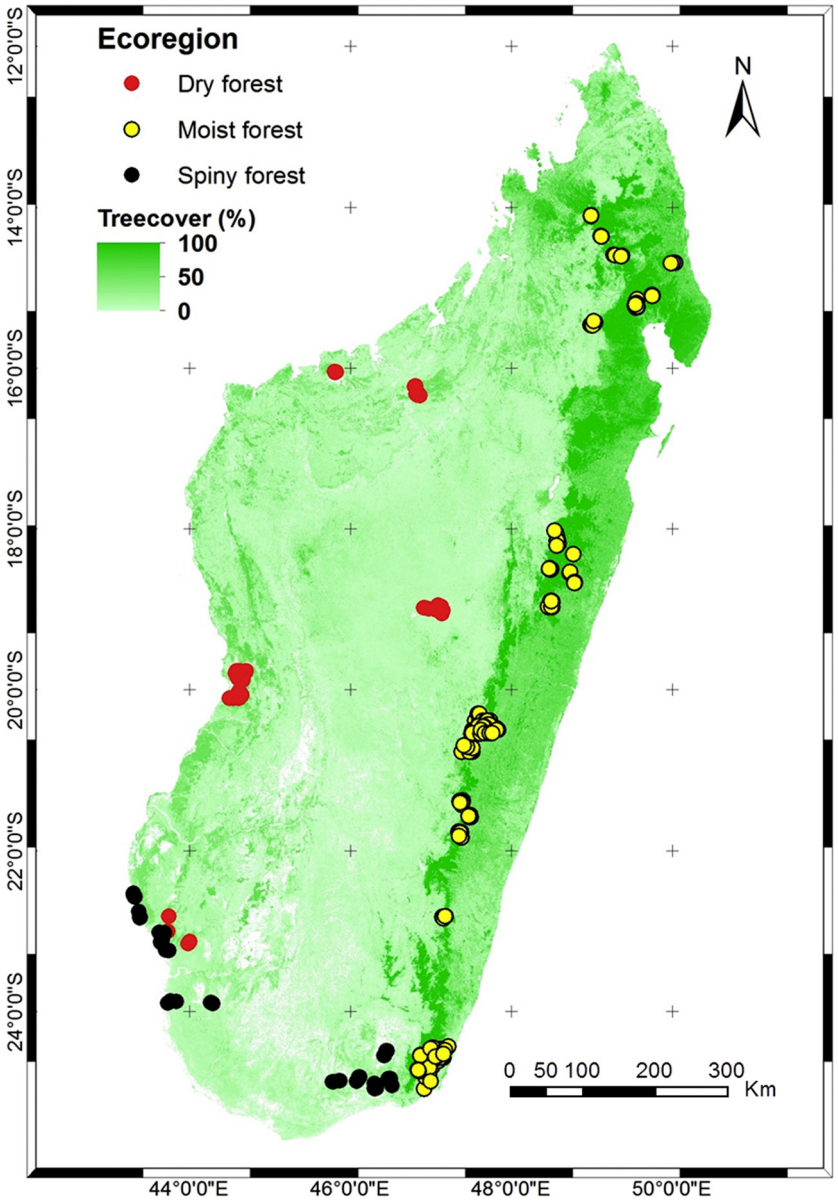

Fig. 1. The study site is the entire island of Madagascar. The background is the Landsat-derived tree cover. Red, yellow and black circles represent field sites in dry forest, moist forest and spiny forest, respectively. (For interpretation of the references to color in this figure legend, the reader is referred to the web version of this article.)

acquisition of data that has allowed the imaging of the planet over time at high resolution. This strategy of systematic acquisition enabled the production by the Japan Aerospace Exploration Agency (JAXA) of mosaic images of up to 25-m resolution (Shimada et al., 2014). These mosaics are radar images preprocessed by the JAXA, made freely available in tiles of 1 degree squared for the years 2007–2010 (Shimada and Ohtaki, 2010). The L-band ALOS PALSAR data have been widely used to estimate the forest biomass. For example, the ALOS PALSAR data were exploited to estimate the biomass of forests threatened by oil palm plantations in Malaysia (Morel et al., 2011), while in Sumatra, texture features from ALOS PALSAR data were used (Thapa et al., 2015). However, estimation of forest biomass using ALOS PALSAR data currently has limitations, because the L-band saturates at about 150 t/ha. Savanna vegetation has lower carbon stocks and is thus more easily estimated with these data. For example, Mermoz et al. (2014) produced a country-level map of Cameroon's savanna biomass at 25-m resolution. In most studies, the cross-polarization (HV) is preferred for estimating biomass because it minimizes the contribution of coupling terms with the ground. Indeed, the HV intensity mainly from the depolarizing part (oriented branches) represents a small proportion of biomass, but it is highly correlated with the total biomass. These studies are based on the fact that the HV intensities are positively correlated with biomass. However, the signal sensitivity decreases as the biomass increases, up to a point called the saturation point, where sensitivity is lost. At L-band HV, this saturation point is about 150 t/ha (Mermoz et al., 2015). After the saturation point, many studies (Woodhouse, 2006; Lucas et al., 2007; Mermoz et al., 2015) have highlighted a weak negative correlation of intensity with biomass. In other words, with high biomass values, the ALOS PALSAR signals decrease. The non-monotonic relationship between intensity and biomass means that corrective models must be established when the range of biomass includes high values. One attempt to retrieve biomass greater than 150 t/ha is the European Space Agency (ESA) P-band BIOMASS mission, to be launched in 2020. Taking advantage of the 300 t/ha saturation point for P-band, this mission aims for more precise measures of global forest biomass (Le Toan et al., 2011; Ho Tong Minh et al., 2015) and hence better

understanding of the terrestrial carbon cycle by measuring global forest biomass.

However, the potential for using L-band radar to estimate high biomass values has not been completely explored. In this study, we propose a new approach to retrieve the full range of biomass using L-band ALOS PALSAR data based on prior knowledge from the global tree cover map at 30-m resolution produced by Hansen et al. (2013). To do this, we use a very large number of forest plots (572) dispersed across Madagascar from 2007 to 2013. Madagascar has a wide variety of forest types (dry forest, spiny forest, and tropical moist forest) known to differ in AGB. It is thus a particularly interesting region for studying spatial variation in the distribution of biomass (and hence of carbon) stocks using radar data.

The paper is organized as follows: in Section 2, the study site is introduced and the proposed methodology is shown; in Section 3, the relationship between radar measurements and AGB is evaluated and the inversion results are presented; in Section 4, we interpret and discuss for each result; in Section 5, we present our conclusions.

2. Data and methods

2.1. Study area

A continental island almost 1600 km long lying off the south-eastern coast of Africa in Indian Ocean, Madagascar stretches between 12° S and 25° S latitude, from Cape Amber in the north to Cape St. Mary in the south, and averages about 500 km in width. Within its area of 587 040 km^2, three types of climates occur. The east coast has a humid tropical climate. West of this coast, the climate is moderate in the north and arid in the south. The broad climatic gradients on the island are associated with elevation and position relative to the dominant south-eastern trade winds (Goodman and Benstead, 2003). Over these climatic gradients occur a large range of tropical forest types, from dry spiny forests in the sub-desert southern regions, to cloud forests at the tops of the northern and eastern mountains. The east coast, exposed to the trade winds, receives the highest rainfall with 3500 mm/year. Forests in the northeast, are particularly wet and lush. Vegetation of western, southern and eastern Madagascar is comprised mainly of dry forest, spiny forest and moist forest, respectively. The moist forests are characterized by dense evergreen vegetation with a canopy exceeding 30 m. Trees of the dry forests shed their leaves in the dry season to limit evapotranspiration, whereas plants of the spiny forests are strongly adapted to drought. Fig. 1 shows the study area and biomass measured in situ.

2.2. Field data

Field data are available from nine forest inventories carried out over the period 1996–2013. Collaboration with different institutions (governmental institutions, conservation NGOs, research institutes) allowed us to obtain data from a large number of forest plots (1771) in the three forest ecoregions of Madagascar (moist, dry and spiny forest ecoregions). However, in this work, we used only the forest inventories from 2007 to 2013 to match with the ALOS PALSAR data, in which 572 plots were selected based on flat field slope and homogeneity within plots. The radius of the plots was 30 m in moist forest (plot size of 0.28 ha) and 20 m in dry or spiny forest (plot size of 0.13 ha). Fig. 2 shows the number of plots and its distribution with respect to each ecoregion. We calculated the AGB biomass (in metric tons) of each tree using the pantropical biomass allometric equation developed by Chave et al. (2014):

$$AGB = 0.0673 \times (\rho \times DBH^2 \times H)^{0.976} \quad (1)$$

where p is the tree wood density in g/cm^3, DBH is the diameter at breast height in cm, H is the tree height in m. Details about the computation of AGB at the plot level are published in Vieilledent et al. (2016).

2.3. Tree cover data

Tree cover data are available globally at 30-m resolution from 2000 to 2012 in Hansen et al. (2013). The primary purpose of that study was to quantify global forest change over the study period. This dataset was obtained by analyzing 654 178 Landsat 7 Enhanced Thematic Mapper Plus scenes, from a total of 1.3 million available. The final results were obtained by training three separate classifiers: one to detect forest loss during the study period, one to detect forest gain during the study period, and one to detect forest cover at the start of the study period. For pixels that were classified as forest loss, the year of loss could essentially be determined by isolating the year of max normalize different vegetation index drop. This resulted in a baseline map of tree cover for the year 2000, forest loss and forest gain during 2001 and 2012. To support our analysis, tree cover maps for Madagascar for 2007, 2008, 2009 and 2010 were generated from the baseline tree cover map of 2000 using the yearly loss/gain information. Detailed discussion of the optical Landsat-derived tree cover dataset can be found in Hansen et al. (2013). In the present study, the dataset for tree cover at 30-m resolution was resampled to 25-m to combine with the SAR data. Fig. 3 shows the distribution of tree cover in 2010 and biomass measured in situ.

2.4. SAR data

520 ALOS PALSAR mosaic tiles with 25-m resolution covering all of Madagascar from 2007 to 2010 were provided freely by the JAXA. Mosaic data are spatially square (1° of latitude and 1° of longitude). The radar signal can be converted into γ^0 values using the following equation:

$$\gamma^0 = 10 \times log10(DN^2) + CF \quad (2)$$

where γ^0 is the normalized intensity, DN is the digital number and CF is the calibration factor, which equals −83.0 as described in Shimada et al. (2014).

The 520 ALOS images used in this study were processed by JAXA using the large-scale mosaicking algorithm described in Shimada and Ohtaki (2010). This algorithm includes ortho-rectification, slope correction and radiometric calibration between neighboring strips. At this stage, the resulting multilook images were perfectly coregistered, and the equivalent number of looks of ALOS PALSAR data was 16. We further improve this four years SAR dataset by exploiting a multi-image filtering developed by Quegan et al. (2000) to reduce noise while retaining as much as possible the fine structures present in the images.

2.5. Proposed methodology for biomass retrieval

Based on results reported from the literature on sensitivity of the L-band intensity in relation to biomass (see Section 1), it is possible to use the L-band HV to estimate biomass for up to a maximum of 150 t/ha. For higher values of biomass, L-band intensity is weakly sensitive variation in biomass. In this section, we present a method to address this problem.

First of all, we propose to weight the radar intensity by the tree cover factor from Section 2.3 using the following formula:

$$\gamma^0_{HVtree} = 10 \times log10(treecover \times DN^2_{HV}) + CF \quad (3)$$

where γ^0_{HVtree} is the intensity weighted by tree cover and the value for tree cover varies from 0 to 1.

Fig. 4 shows the distribution of γ^0_{HV}, γ^0_{HVtree} and biomass measured in situ, for the year 2010. A significant growth was observed in intensity with low biomass levels, followed by a loss of sensitivity and a slight decrease in signal intensity beginning at 150 t/ha. The range of γ^0_{HVtree} is much higher than that of γ^0_{HV}. In the high range of biomass values, there is no difference between the sensitivity of γ^0_{HV} and γ^0_{HVtree}. In fact, as seen in Fig. 3, we found that of plots where biomass was greater than 150 t/

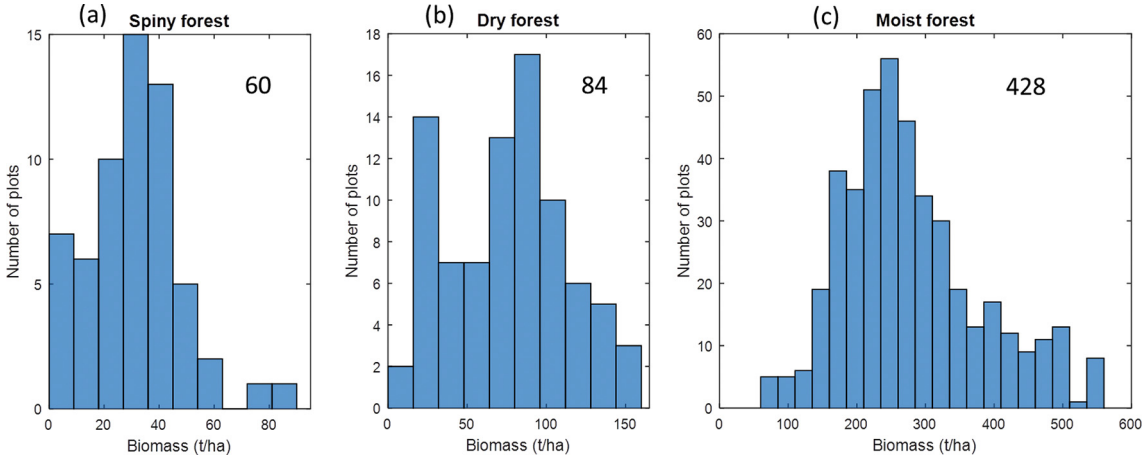

Fig. 2. Biomass measured in situ in spiny (a), dry (b) and moist (c) forest ecoregions. Number of plots sampled were 60, 84 and 428, respectively.

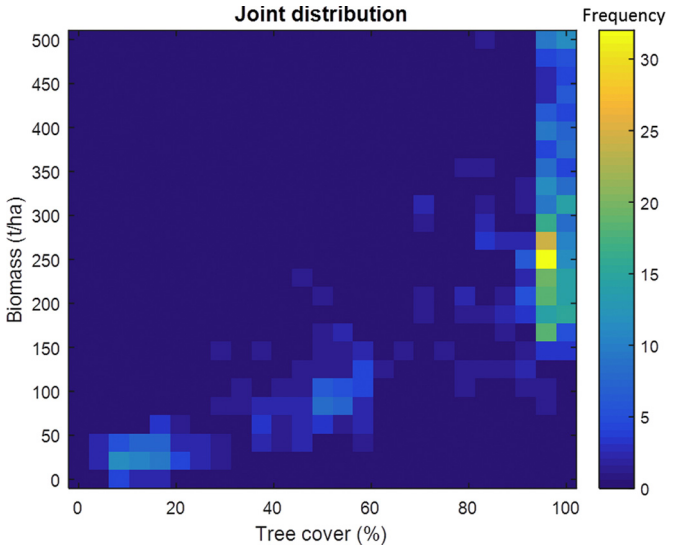

Fig. 3. The joint distribution between Landsat-derived tree cover and biomass measured in situ. More than 98% of plots with AGB > 150 t/ha had tree cover of 95% or greater.

ha, 98% had tree cover of 95% or more. Based on this observation, we proposed to use tree cover of 95% as a threshold to recognize the high range of biomass values.

To highlight the usefulness of γ^0_{HVtree} in our approach, we compare the sensitivity of γ^0_{HV} (unweighted radar intensity), γ^0_{HVtree} (radar intensity weighted by tree cover) and tree cover with in situ biomass values in the low range (e.g., < 150 t/ha) in Fig. 5. The highest correlation is observed with the weighted radar intensity data. The γ^0_{HV} data exhibit a much lower sensitivity to biomass ($R^2 = 0.34$) than do the γ^0_{HVtree} data ($R^2 = 0.77$). One possible explanation of this result is that radar intensity integrates noise signals from the ground and this problem can be partly mitigated by incorporating tree cover data from optical images. Finally, by comparing γ^0_{HVtree} and tree cover in Fig. 5b and c, the γ^0_{HVtree} data exhibit a higher sensitivity to biomass ($R^2 = 0.77$ versus 0.72) and a smaller root mean square error (RMSE) (26% versus 30%).

For biomass lower than 150 t/ha, we fit an exponential model to link radar signal to biomass (Mitchard et al., 2011), described as

$$\gamma^0_{HVtree} = a + b \times (1 - e^{-c \times AGB}) \quad (4)$$

where AGB is the biomass measured in situ, a, b and c are coefficients to be estimated from the data.

For higher values of biomass, we fitted a linear model (Mermoz et al., 2015), described as

$$\gamma^0_{HVtree} = m + n \times AGB \quad (5)$$

where m and n are coefficients to be estimated from the data.

By using Eqs. (4) and (5), an estimation of biomass $\widehat{AGB}$ can be calculated from γ^0_{HVtree}. However, in our approach, a bias in the inversion can be introduced. In the statistical literature, this phenomenon is

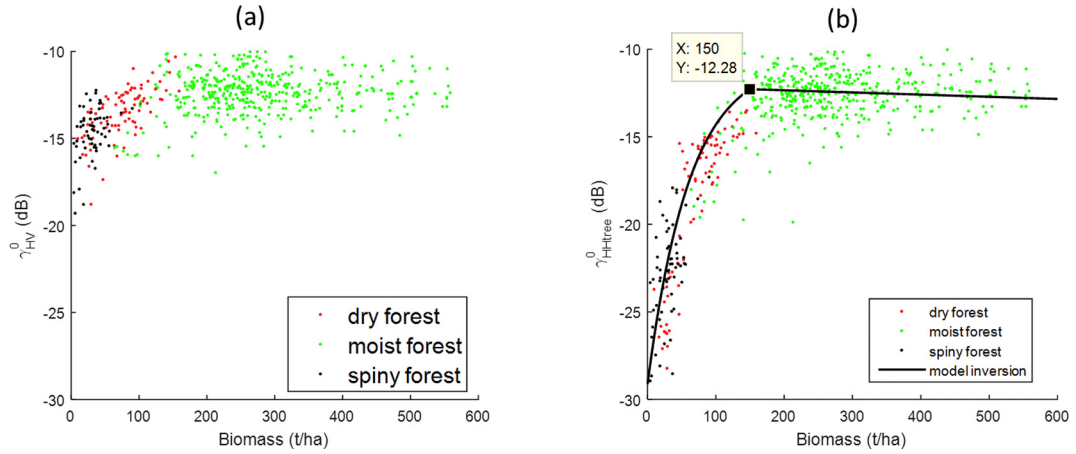

Fig. 4. (a) Biomass measured in situ versus γ^0_{HV}. (b) Biomass measured in situ versus γ^0_{HVtree}.

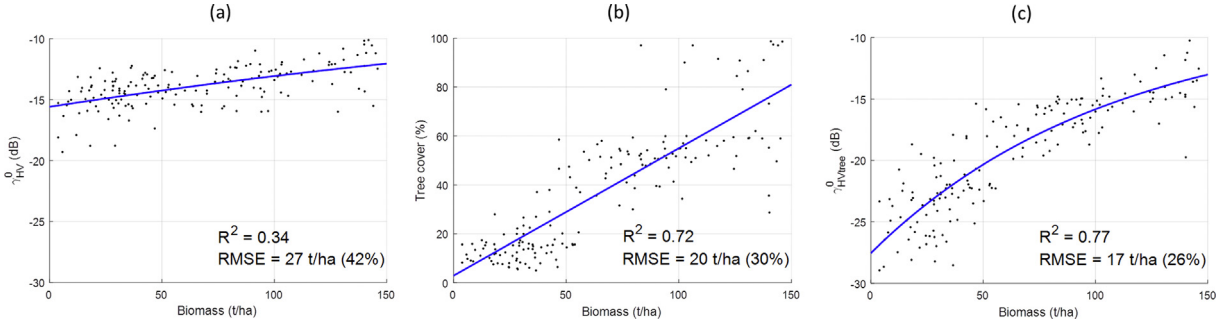

Fig. 5. (a) Biomass measured in situ versus γ^0_{HV}. (b) Biomass measured in situ versus tree cover. (c) Biomass measured in situ versus γ^0_{HVtree}. The blue line is the best fit of the data. (For interpretation of the references to color in this figure legend, the reader is referred to the web version of this article.)

referred to as regression dilution, in that random error in the independent variable leads to systematic underestimation of the regression slope (Fuller, 1987; Frost and Thompson, 2000). To correct for such bias, we compensate the biomass by a ratio β, described as

$$Bias\,[\widehat{AGB}] = \beta \times AGB \tag{6}$$

where $Bias\,[\widehat{AGB}] = E\,[\widehat{AGB} - AGB]$ and $E(\cdot)$ denotes expected operator, i.e., averaging over a number of observations.

2.6. Calibration for Madagascar

A common method for biomass retrieval is to exploit an inverse model based on the empirical regression derived from the available set of in situ and radar plot data. In this work, using 572 biomass plots for fitting with each year's SAR data, e.g. for the year 2010, we found that

For biomass lower than 150 t/ha:

$$\widehat{AGB} = -\frac{1}{c} \times ln\left(1 - \frac{\gamma^0_{HVtree} - a}{b}\right) \tag{7}$$

With $a = -29.13 \pm 0.09$, $b = 18.47 \pm 0.14$ and $c = 0.01623 \pm 0.00034$. In the low range of biomass values, γ^0_{HVtree} is very highly correlated with biomass ($R^2 = 0.77$ and $p < 10^{-5}$).

For higher biomass values and tree cover greater than 95%:

$$\widehat{AGB} = \frac{\gamma^0_{HVtree} - m}{n} \tag{8}$$

With $m = -12.14 \pm 0.28$ and $n = -9.28.10^{-4} \pm 9.35.10^{-5}$. In the high range of biomass values, γ^0_{HVtree} is less strongly correlated with biomass ($R^2 = 0.18$ and $p = 0.017$).

Fig. 4b plots Eqs. (7) and (8), showing the fit between the weight the radar intensity and the in situ biomass.

Finally, the estimated biomass can be calculated as

$$Biomass = (1 + \beta) \times \widehat{AGB} \tag{9}$$

With $\beta = 0.2392 \pm 0.0515$.

2.7. Carbon estimation and uncertainty

The calibration described in Section 2.6 allows estimation of aboveground biomass in Madagascan forests. To calculate carbon stock, we convert biomass into carbon units using the 0.47 ratio (Vieilledent et al., 2016). We apply a filter to this carbon data based on the tree cover map and only include pixels with > 25% tree cover. In others words, we follow a conservative approach in defining forest: only land with tree cover not less than 25% was considered as forest (Hansen et al., 2013; Shimada et al., 2014).

The model inversion between biomass and radar is affected by the uncertainties in radar signal, tree cover estimate and in situ biomass data. The radar signal is impacted by a number of factors related to forest structure and environments. The signal can also be affected by variation in the performance of the signal emitter over time. However, the ALOS PALSAR γ^0_{HV} was found to be very stable at 0.065 dB over its lifetime 2006–2010 (Shimada et al., 2014). Regarding the tree cover dataset, there is little uncertainty, with classification error less than 1% (Hansen et al., 2013). Regarding in situ biomass measurements, the data collection procedures in the sources we used varied somewhat across organizations, but all the different protocols allowed estimating biomass in t/ha at the center of each forest plot. Application of an uncertainty analysis at each stage is out of the scope of this study. If all sources of uncertainties can be estimated, an explicit equation can be applied to ALOS PALSAR data (Mermoz et al., 2014). Nonetheless, in this work, uncertainties related to the carbon estimates are estimated by Monte Carlo simulations. Such uncertainties affect the definition of the inverse model (imprecision and bias), as the in situ biomass estimates are used to fit parameters of the model. A new inverse model is derived by estimating the coefficients(a, b, c, m, n, β) and biomass is estimated at each generation (with 1000 realisations). For each pixel, the dispersion of biomass values resulting from the 1000 possible models is used to calculate the standard deviation in the uncertainty associated with the estimation of biomass (and hence of carbon).

3. Results

The methods proposed in Section 2.5 were applied to ALOS PALSAR data in Madagascar. The RMSE and the correlation R^2 were used to evaluate performance of the SAR dataset for each year using all in situ plots available. The same performance for biomass retrieval with respect to in situ data was found for all four years. The results, presented in Fig. 6a, showed a RMSE of 30% (for biomass ranging from 0 to 500 t/ha) and $R^2 = 0.71$, for the year 2010. To avoid overfitting, we carried out a 10-fold cross-validation procedure (McLachlan et al., 2005). For biomass values in the range 0–150 t/ha, the average RMSE in 2010 was 26% and $R^2 = 0.77$, whereas for biomass values in the range 0–300 t/ha in the same year, the average RMSE was 28% and $R^2 = 0.72$.

Second, 520 ALOS PALSAR 25-m resolution images were used to retrieve biomass for 2007, 2008, 2009 and 2010. The biomass maps for these four years were found to be similar in their biomass content. An example of the biomass map for 2010 is shown in Fig. 7b. To appreciate the 25-m pixel size of the biomass map, a zoom version in an $0.5^\circ \times 0.5^\circ$ window was shown in the bottom. The distribution of biomass at 25-m resolution shows details of spatial biomass density, indicating a west-east gradient.

Third, using our map at 25-m resolution, we estimated the forest carbon stocks for dry, spiny and moist ecoregions, respectively (see Table 1). The total forest carbon in the four years 2007, 2008, 2009 and 2010 is 1.1173 ± 0.0304, 1.1029 ± 0.0303, 1.0916 ± 0.0301 and 1.0773 ± 0.0298 PgC (1 PgC = 10^{15} g carbon), respectively. Over the four years carbon stocks were found to have decreased by approximately 0.01 PgC/year. Finally, using the carbon map in 2007 and in 2010, we established the forest carbon change over the period

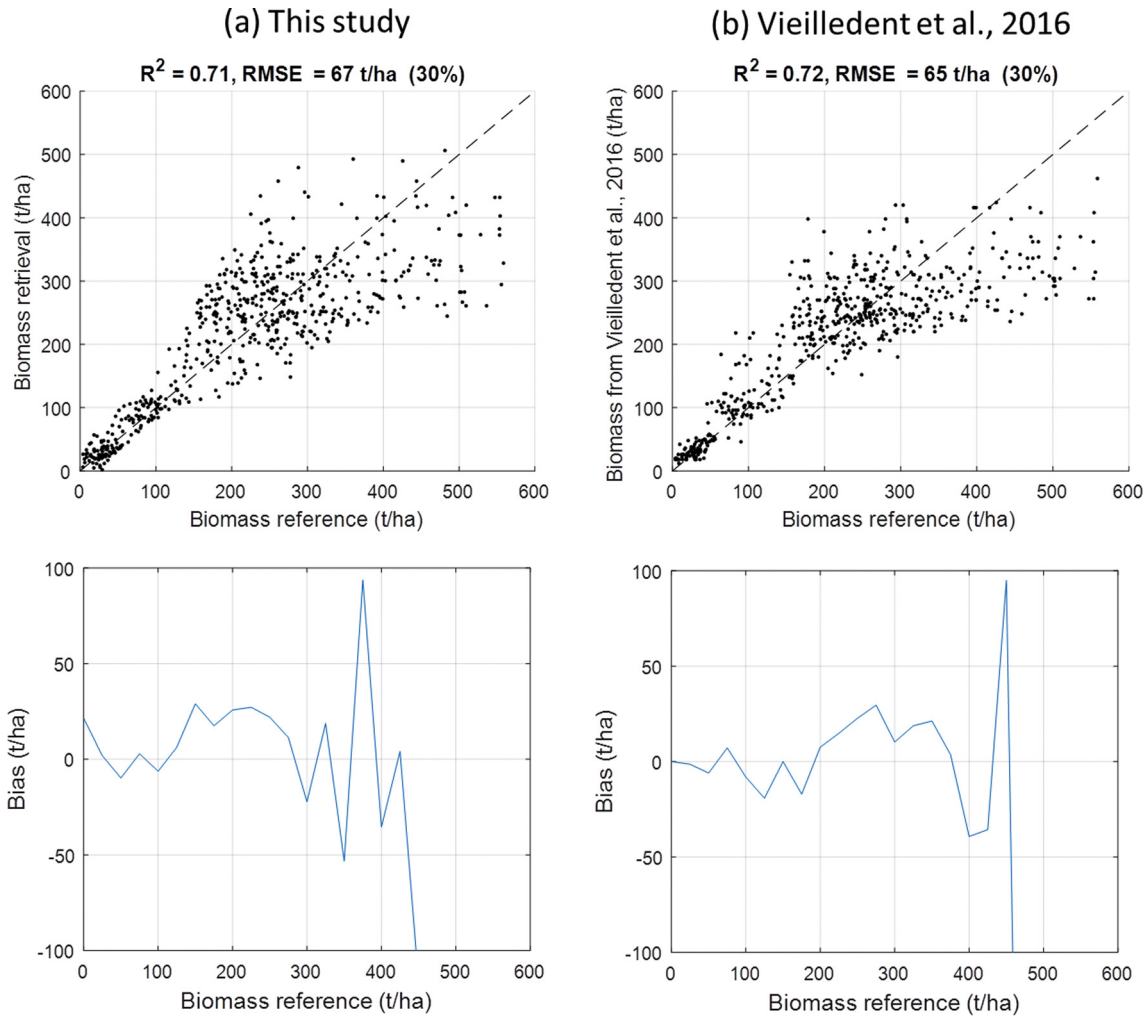

Fig. 6. (a) The biomass inversion performance of this study. (b) Performance in the study of Vieilledent et al. (2016). Top panels are the cross-plot 1:1. Bottom panels are the bias. The biomass retrieval appears to be reliable for biomass ranging from 0 to 300 t/ha.

2007–2010 (see Fig. 8).

4. Discussions

In this work we show that radar signal intensity combined with tree cover data can be used to estimate biomass across the entire range of biomass values in Madagascan forests. As seen in Fig. 5, weighting the radar signal by tree cover data increased the correlation between the radar signal and biomass. The weighted radar intensity follows a logarithmic regression and biomass reaches a certain threshold at which the signal becomes saturated and then quickly decreases. The present analysis confirms the possibility of exploiting such behavior in an inversion scheme to retrieve the full range of biomass up to 500 t/ha. Relative error in performance of biomass retrieval was 30% and the correlation between the weighted radar intensity and biomass was high (R^2 = 0.71) at 25-m resolution. Finally, we showed that biomass can be mapped efficiently even in tropical dense forests. Together, these results considerably add to our confidence in the ability of current and future missions such as L-band ALOS-2, L-band SAOCOM and P-band BIOMASS to provide accurate wall-to-wall biomass mapping. In particular, the arrival of the P-band sensor BIOMASS, which will exploit a volume layer through tomographic processing (Ho Tong Minh et al., 2014), will make it possible to estimate forest biomass with relative error of only about 11% at 4-ha resolution (Ho Tong Minh et al., 2015, 2016).

First, we showed that the inversion method described in Section 2.5 can be applied to retrieve the full range of biomass values. Our analysis was successfully conducted for forests of the entire island of Madagascar. It is worth noting that the inversion for high range of biomass values (e.g. greater than 150 t/ha) is mainly based on the fact that L-band radar signal decreases with increasing height of forest vegetation, a phenomenon that is well-known in the L-band literature (Woodhouse, 2006; Lucas et al., 2007; Mermoz et al., 2015). In addition, even at the longer wavelength P-band (wavelength 69 cm), the relationship between the ground layer and biomass exhibits a negative trend (Ho Tong Minh et al., 2014), similar to that observed for the L-band. The decrease can be explained by signal extinction, which likely to be higher in the presence of tall trees (and hence of high biomass).

To place this result in perspective, we compared our analysis with the work of Vieilledent et al. (2016). Their map was generated by using a correlative approach based on a bioclimatic envelope model and data from all 1771 forest plots inventoried during the period 1996–2013 over a large climatic gradient. The reader is referred to Vieilledent et al. (2016) for details. In fact, Vieilledent's map is represented as the most accurate biomass map available at 250-m resolution for the year 2010 in Madagascar. The comparisons are shown in Figs. 6 and 7. For the year 2010, from Fig. 6, the correlation R^2 and relative error are quite similar between the two maps. However, thanks to the 25-m resolution of the ALOS PALSAR data, our map of biomass distribution is more detailed than Vieilledent's map at 250-m resolution (see Fig. 7). For

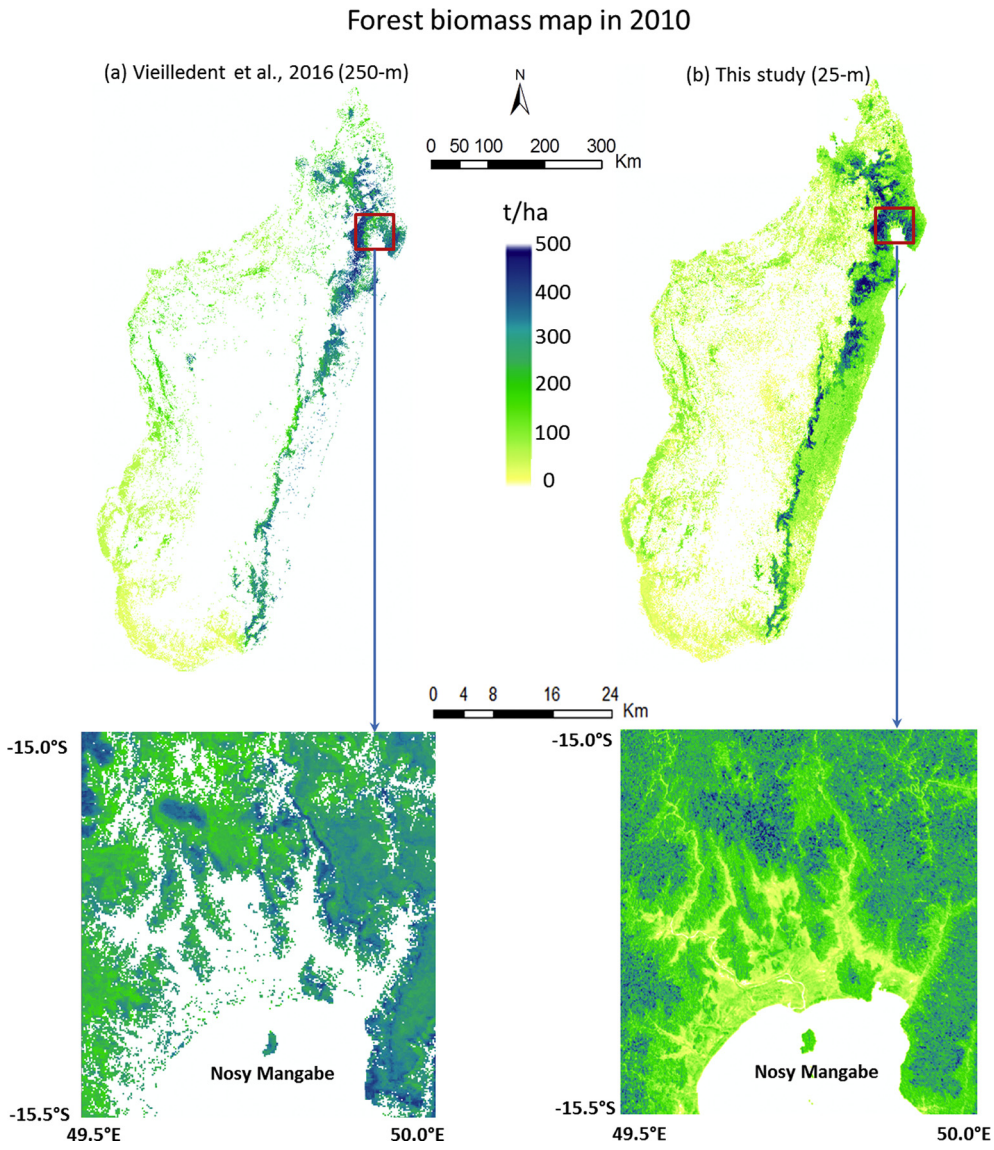

Fig. 7. Biomass maps for Madagascan forests for the year 2010 are shown. The color scale varying from yellow to green to blue illustrates the full biomass range from 0 to 500 t/ha. The spatial distribution of biomass for the entire island of Madagascar shows a west-east gradient. (a) Map from the study of Vieilledent et al. (2016) and (b) map from this work. The bottom panels show a zoom version of red-bordered boxes to facilitate visualization of the biomass results. (For interpretation of the references to color in this figure legend, the reader is referred to the web version of this article.)

example, in the bottom panels of Fig. 7, our map shows details of savanna ecosystems close to the coast such as forest savanna, woody savanna, and gallery forests, whereas in Vieilledent's map, they cannot be shown, owing to the limitation of the data available in the bioclimatic envelope model (Vieilledent et al., 2016). Furthermore, it is worth pointing out that if we only consider the low range of biomass values (i.e., < 150 t/ha), our result is slightly better than that of Vieilledent (R^2 = 0.77 versus 0.76 and *RMSE* = 26% versus 31%). This is important because almost 80% of forest cover of Madagascar has biomass values less than 150 t/ha.

Third, we calculated that the values for total forest carbon in 2010 was 1.0773 ± 0.0298 PgC, whereas by using Vieilledent's map at 250-m resolution, it was 0.8738 PgC. It is worth recalling the results of others studies, for example those of Saatchi et al. (2011) and Baccini et al. (2012). These results were predicted for the year 2010 by Vieilledent et al. (2016) as 0.7490 PgC and 0.6392 PgC for Saatchi's and

Table 1
Surface area (ha) and carbon assessment (PgC) in Madagascar with respect to the dry, spiny and moist forest ecoregions.

	2007		2008		2009		2010	
	Area (ha)	Carbon (PgC)	Area (ha)	Carbon (PgC)	Area (ha)	Carbon (PgC)	Area (ha)	Carbon (PgC)
Dry	4,770,533	0.1635 ± 0.0078	4,725,042	0.1623 ± 0.0079	4,695,772	0.1601 ± 0.0079	4,639,216	0.1528 ± 0.0076
Spiny	355,857	0.0112 ± 0.0011	352,230	0.0111 ± 0.0011	346,299	0.0108 ± 0.0011	341,805	0.0104 ± 0.0011
Moist	13,263,951	0.9426 ± 0.0215	13,228,492	0.9295 ± 0.0213	13,193,701	0.9207 ± 0.0211	13,147,997	0.9141 ± 0.0211
Total	18,390,341	1.1173 ± 0.0304	18,305,764	1.1029 ± 0.0303	18,235,772	1.0916 ± 0.0301	18,129,018	1.0773 ± 0.0298

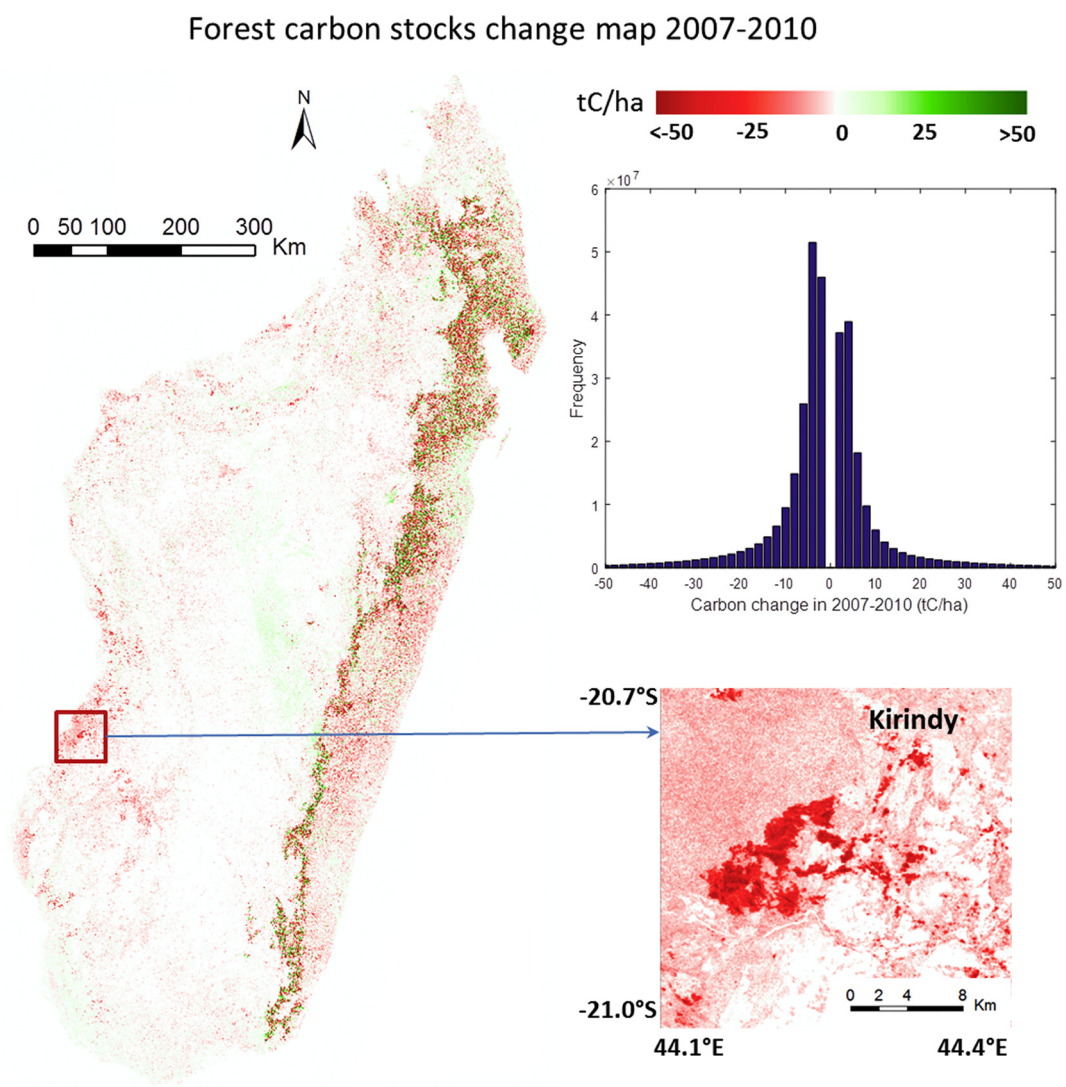

Fig. 8. Map of change in Madagascar forest carbon stocks in the period 2007–2010. A zoom version of the red-bordered box is provided to facilitate visualization of the carbon loss in Kirindy. The top right panel is the histogram showing distribution of values, excluding values of zero. (For interpretation of the references to color in this figure legend, the reader is referred to the web version of this article.)

Baccini's, respectively. In all cases, we found that their results were underestimated for the total forest carbon stocks, owing to the low resolution of the maps used, with pixel size ranging from 250 m (Vieilledent) to 500 m (Baccini) to 1000 m (Saatchi) and to the limitation of the data in the model inversion, where missing data was treated as zeros. In our estimation, carbon stocks tended to decrease over 2007–2010 by approximately 0.01 PgC/year, caused by anthropogenic deforestation and probably climate change, both of which are known or suspected to lead to decrease carbon stocks in tropical forests elsewhere (Vieilledent et al., 2016). As shown by Fig. 8, most of the affected areas nationally are in areas of tropical moist forests, i.e., in the east of the island (see also Table 1). Indeed, in Madagascar, around 57 000 ha were deforested each year in the period 2000–2010(see Vieilledent et al., 2018). Assuming a mean carbon stock of 100 tC/ha, we obtain an annual carbon loss of 0.006 PgC. The difference (0.004 PgC) could be attributed to degradation (caused by direct human actions, climatic events or both).

Finally, to highlight our results on changes in carbon stocks, Fig. 8 includes a zoom of an area (outlined in red) near Kirindy. This area of strong carbon stock loss is associated with deforestation, caused by the cyclone Fanele in 2009 followed by uncontrolled fires in the following years (Lewis and Bannar-Martin, 2012). In addition, for each year in Madagascar, the forest carbon gain is usually < 5 tC/year (Fox et al., 2011; Poorter et al., 2016), equivalent to < 15 tC for the three-year period 2007–2010. Interestingly, this was confirmed by the histogram in Fig. 8, showing very few pixels with values of carbon change over 15 tC/ha.

5. Conclusions

In this study, we have developed a methodology for retrieving the full range of forest biomass values in Madagascar. The methods are based on 572 forest plots and 520 ALOS PALSAR mosaic tiles with 25-m resolution acquired from 2007 to 2010 over the entire island. The method improved the biomass inversion by combining radar intensity and data on tree cover, which resulted in increasing the correlation between the radar signal and biomass. The correlation between the radar signal and biomass measured in situ was high (R^2 = 0.71), and the RMSE was 30% (for biomass ranging from 0 to 500 t/ha). For the low range of biomass values (e.g., < 150 t/ha), the correlation was higher (R^2 = 0.77, *RMSE* = 26%). The ALOS PALSAR mosaic data from all of Madagascar were inverted into biomass values. The spatial distribution of biomass at 25-m resolution for the entire island shows a west-east gradient. The biomass map also shows details of savanna

ecosystems close to the coast such as forest savanna, woody savanna, and gallery forests. Over 2007–2010 period, carbon stocks were found to have decreased constantly, owing to anthropogenic deforestation and probably to climate change. We expect these results to serve as a more accurate benchmark than the heretofore state-of-the-arts results of Saatchi et al. (2011), Baccini et al. (2012), and Vieilledent et al. (2016). Our results reinforce the science basis for current and future missions such as ALOS-2, SAOCOM and BIOMASS, increasing our confidence that they can provide accurate wall-to-wall biomass mapping, and thereby enabling progress on REDD initiatives. Combining radar signal with optical tree cover data appears to be a promising approach for using by L-band SAR to map forest biomass (and hence carbon) over broad geographical scales.

Acknowledgments

This work was supported in part by the Programme National de Teledetection Spatiale (PNTS, http://www.insu.cnrs.fr/pnts), project no. PNTS-2016-06. Ghislain Vieilledent was supported by the FRB-FFEM-BioSceneMada project (project agreement AAP-SCEN-2013I) and the ReCaREDD European Commission project. We thank the government of Burundi for funding the PhD research of Emile Ndikumana. ALOS PALSAR images were provided by the Japan Aerospace Exploration Agency.

References

Baccini, A., Goetz, S.J., Walker, W.S., Laporte, N.T., Sun, M., Sulla-Menashe, D., Hackler, J., Beck, P.S.A., Dubayah, R., Friedl, M.A., Samanta, S., Houghton, R.A., 2012. Estimated carbon dioxide emissions from tropical deforestation improved by carbon-density maps. Nat. Clim. Chang. 2 (3), 182–185.

Chave, J., Rejou-Machain, M., Burquez, A., Chidumayo, E., Colgan, M.S., Delitti, W.B., Duque, A., Eid, T., Fearnside, P.M., Goodman, R.C., Henry, M., Martinez-Yrizar, A., Mugasha, W.A., Muller-Landau, H.C., Mencuccini, M., Nelson, B.W., Ngomanda, A., Nogueira, E.M., Ortiz-Malavassi, E., Pelissier, R., Ploton, P., Ryan, C.M., Saldarriaga, J.G., Vieilledent, G., 2014. Improved allometric models to estimate the aboveground biomass of tropical trees. Glob. Chang. Biol. 20 (10), 3177–3190. http://dx.doi.org/10.1111/gcb.12629.

Dobson, M., Ulaby, F., LeToan, T., Beaudoin, A., Kasischke, E., Christensen, N., 1992. Dependence of radar backscatter on coniferous forest biomass. IEEE Trans. Geosci. Remote Sens. 30 (2), 412–415 (Mar).

Fox, J.C., Vieilledent, G., Yosi, C.K., Pokana, J.N., Keenan, R.J., 2011. Aboveground forest carbon dynamics in Papua New Guinea: isolating the influence of selective-harvesting and El Nino. Ecosystems 14 (8), 1276–1288. http://dx.doi.org/10.1007/s10021-011-9480-4.

Frost, C., Thompson, S.G., 2000. Correcting for regression dilution bias: comparison of methods for a single predictor variable. J. R. Stat. Soc. 163 (2), 173–189.

Fuller, W.A. (Ed.), 1987. Measurement Error Models. John Wiley, New York.

Goodman, S., Benstead, J. (Eds.), 2003. The Natural History of Madagascar. University of Chicago Press.

Hansen, M.C., Potapov, P.V., Moore, R., Hancher, M., Turubanova, S.A., Tyukavina, A., Thau, D., Stehman, S.V., Goetz, S.J., Loveland, T.R., Kommareddy, A., Egorov, A., Chini, L., Justice, C.O., Townshend, J.R.G., 2013. High-resolution global maps of 21st-century forest cover change. Science 342 (6160), 850–853.

Ho Tong Minh, D., Le Toan, T., Rocca, F., Tebaldini, S., Mariotti d'Alessandro, M., Villard, L., 2014. Relating P-band synthetic aperture radar tomography to tropical forest biomass. IEEE Trans. Geosci. Remote Sens. 52 (2), 967–979 (Feb).

Ho Tong Minh, D., Le Toan, T., Rocca, F., Tebaldini, S., Villard, L., Rejou-Mechain, M., Phillips, O.L., Feldpausch, T.R., Dubois-Fernandez, P., Scipal, K., Chave, J., 2016. SAR tomography for the retrieval of forest biomass and height: cross-validation at two tropical forest sites in French Guiana. Remote Sens. Environ. 175, 138–147 (Mar).

Ho Tong Minh, D., Tebaldini, S., Rocca, F., Le Toan, T., Villard, L., Dubois-Fernandez, P., 2015, Feb, Feb. Capabilities of BIOMASS tomography for investigating tropical forests. IEEE Trans. Geosci. Remote Sens. 53 (2), 965–975.

Hufty, M., Haakenstad, A., 2011. Reduced emissions for deforestation and degradation - a critical review. J. Sustain. Dev. 5 (1), 1–24.

Le Toan, T., Beaudoin, A., Riom, J., Guyoni, D., 1992. Relating forest biomass to SAR data. IEEE Trans. Geosci. Remote Sens. 30 (2), 403–411 (Mar).

Le Toan, T., Quegan, S., Davidson, M., Balzter, H., Paillou, P., Papathanassiou, K., Plummer, S., Rocca, F., Saatchi, S., Shugart, H., Ulander, L., 2011. The BIOMASS mission: mapping global forest biomass to better understand the terrestrial carbon cycle. Remote Sens. Environ. 2850–2860 (Jun).

Lewis, R.J., Bannar-Martin, K.H., 2012. The impact of cyclone fanele on a tropical dry forest in Madagascar. Biotropica 44, 135–140.

Lucas, R.M., Mitchell, A.L., Rosenqvist, A., Proisy, C., Melius, A., Ticehurst, C., 2007. The potential of l-band SAR for quantifying mangrove characteristics and change - case studies from the tropics. Aquat. Conserv. Mar. Freshwat. Ecosyst. 17 (1), 245–264.

McLachlan, G.J., Do, K.-A., Ambroise, C. (Eds.), 2005. Analyzing Microarray Gene Expression Data. John Wiley, New York.

Mermoz, S., Rejou-Mechain, M., Villard, L., Toan, T.L., Rossi, V., Gourlet-Fleury, S., 2015. Decrease of l-band {SAR} backscatter with biomass of dense forests. Remote Sens. Environ. 159 (0), 307–317. http://www.sciencedirect.com/science/article/pii/S0034425714005112.

Mermoz, S., Toan, T.L., Villard, L., Réjou-Méchain, M., Seifert-Granzin, J., 2014. Biomass assessment in the Cameroon savanna using ALOS PALSAR data. Remote Sens. Environ. 155, 109–119. http://www.sciencedirect.com/science/article/pii/S0034425714001540.

Mitchard, E., Saatchi, S., Lewis, S., Feldpausch, T., Woodhouse, I., Sonké, B., Rowland, C., Meir, P., 2011. Measuring biomass changes due to woody encroachment and deforestation/degradation in a forest savanna boundary region of central Africa using multi-temporal L-band radar backscatter. Remote Sens. Environ. 115 (11), 2861–2873. http://www.sciencedirect.com/science/article/pii/S0034425711001337 {DESDynI} VEG-3D Special Issue.

Morel, A.C., Saatchi, S.S., Malhi, Y., Berry, N.J., Banin, L., Burslem, D., Nilus, R., Ong, R.C., 2011. Estimating aboveground biomass in forest and oil palm plantation in Sabah, Malaysian Borneo using {ALOS} {PALSAR} data. For. Ecol. Manag. 262 (9), 1786–1798. http://www.sciencedirect.com/science/article/pii/S0378112711004361.

Pan, Y., Birdsey, R.A., Fang, J., Houghton, R., Kauppi, P.E., Kurz, W.A., Phillips, O.L., Shvidenko, A., Lewis, S.L., Canadell, J.G., Ciais, P., Jackson, R.B., Pacala, S.W., McGuire, A.D., Piao, S., Rautiainen, A., Sitch, S., Hayes, D., 2011. A large and persistent carbon sink in the world's forests. Science 333, 988–993.

Poorter, L., Bongers, F., Aide, T., Zambrano, A.A., Balvanera, P., Becknell, J., Boukili, V., Brancalion, P., Broadbent, E., Chazdon, R., Craven, D., de Almeida-Cortez, J., Cabral, G., de Jong, B., Denslow, J., Dent, D., DeWalt, S., Dupuy, J., Duran, S., Espirito-Santo, N., Fandino, M., Czsar, R., Hall, J., Hernandez-Stefanoni, J., Jakovac, C., Junqueira, A., Kennard, D., Letcher, S., Licona, J., Lohbeck, M., Marin-Spiotta, E., Martinez-Ramos, M., Massoca, P., Meave, J., Mesquita, R., Mora, F., Munoz, R., Muscarella, R., Nunes, Y., Ochoa-Gaona, S., de Oliveira, A., Orihuela-Belmonte, E., Pena-Claros, M., Perez-Garcia, E., Piotto, D., Powers, J., Rodriguez-Velazquez, J., Romero-Perez, I., Ruiz, J., Saldarriaga, J., Sanchez-Azofeifa, A., Schwartz, N., Steininger, M., Swenson, N., Toledo, M., Uriarte, M., van Breugel, M., van der Wal, H., Veloso, M., Vester, H., Vicentini, A., Vieira, I., Bentos, T.V., Williamson, G., Rozendaal, D., 2016. Biomass resilience of neotropical secondary forests. Nature 530, 211–214 (Feb).

Quegan, S., Le Toan, T., Yu, J.J., Ribbes, F., Floury, N., 2000, Mar, Mar. Multitemporal ERS SAR analysis applied to forest mapping. IEEE Trans. Geosci. Remote Sens. 38 (2), 741–753.

Saatchi, S.S., Harris, N.L., Brown, S., Lefsky, M., Mitchard, E.T.A., Salas, W., Zutta, B.R., Buerman, W., Lewis, S.L., Hagen, S., Petrova, S., White, L., Silman, M., Morel, A., 2011. Benchmark map of forest carbon stocks in tropical regions across three continents. Proc. Natl. Acad. Sci. U. S. A. 108 (24), 9899–9904 (Jun).

Shimada, M., Itoh, T., Motooka, T., Watanabe, M., Shiraishi, T., Thapa, R., Lucas, R., 2014. New global forest/non-forest maps from ALOS PALSAR data (2007–2010). Remote Sens. Environ. 155, 13–31. http://www.sciencedirect.com/science/article/pii/S0034425714001527.

Shimada, M., Ohtaki, T., 2010, Dec, Dec. Generating large-scale high-quality sar mosaic datasets: application to palsar data for global monitoring. IEEE J. Sel. Top. Appl. Earth Obs. Remote Sens. 3 (4), 637–656.

Thapa, R.B., Watanabe, M., Motohka, T., Shimada, M., 2015. Potential of high-resolution ALOS PALSAR mosaic texture for aboveground forest carbon tracking in tropical region. Remote Sens. Environ. 160, 122–133. http://www.sciencedirect.com/science/article/pii/S0034425715000164.

Vieilledent, G., Gardi, O., Grinand, C., Burren, C., Andriamanjato, M., Camara, C., Gardner, C., Glass, L., Rasolohery, A., Ratsimba, H., Gond, V., Rakotoarijaona, J., 2016. Bioclimatic envelope models predict a decrease in tropical forest carbon stocks with climate change in Madagascar. J. Ecol. 104 (3), 703–715 (may).

Vieilledent, G., Grinand, C., Rakotomalala, F.A., Ranaivosoa, R., Rakotoarijaona, J.-R., Allnutt, T.F., Achard, F., 2018. Combining global tree cover loss data with historical national forest-cover maps to look at six decades of deforestation and forest fragmentation in Madagascar. Biol. Conserv. 222, 189–197. http://dx.doi.org/10.1016/j.biocon.2018.04.008.

Woodhouse, I.H., 2006. Predicting backscatter-biomass and height-biomass trends using a macroecology model. IEEE Trans. Geosci. Remote Sens. 44 (4), 871–877 (April).